IRAS[1] OBSERVATIONS OF THE DIFFUSE INFRARED BACKGROUND

M. G. HAUSER, F. C. GILLETT, F. J. LOW, T. N. GAUTIER, C. A. BEICHMAN, G. NEUGEBAUER, H. H. AUMANN,
B. BAUD, N. BOGGESS, J. P. EMERSON, J. R. HOUCK, B. T. SOIFER, AND R. G. WALKER

ABSTRACT

IRAS data reveal bright emission from interplanetary dust which dominates the celestial background at 12, 25, and 60 μm except near the galactic plane. At 100 μm, interplanetary dust emission is prominent only near the ecliptic plane; diffuse galactic emission is found over the rest of the sky. At the galactic poles, the observed brightness implies that A_v is likely to be of order 0.1 mag. The angular variation of the zodiacal emission in the ecliptic plane and in the plane at elongation 90°, and an annual modulation of the ecliptic pole brightness, are generally consistent with previously determined interplanetary dust distributions.

Subject headings: infrared: general — interplanetary medium — interstellar: grains

I. INTRODUCTION

The diffuse infrared background is of astrophysical interest because of what it can reveal about the solar system, the interstellar medium, and the universe on large scales. Measurements of this emission have been made from rocket-borne instruments (Soifer, Houck, and Harwit 1971; Briotta 1976; Price, Murdock, and Marcotte 1980). In this *Letter* we describe the large-scale features of the diffuse infrared background determined from initial *IRAS* survey data. A preliminary separation of the emission into its solar system (zodiacal emission, ZE) and galactic components is made.

II. OBSERVATIONAL METHODS AND RESULTS

The *IRAS* mission, instruments, and calibration procedures are described by Neugebauer *et al.* (1984, hereafter Paper I). For study of the background, the survey data in each band have been averaged over all detectors and over 8 s of time, giving samples with one-half degree spacing. The survey scan geometry is particularly convenient for studying the ZE, since each scan is done at a fixed solar elongation.

Absolute radiometry with the survey array is possible because the signals are DC-coupled, the electronic baselines remain stable on time scales of hours, and the zero point is determined experimentally. The system responsivity for each detector channel and the effective beam sizes were determined from scans of known sources (Paper I). Two methods were used to establish the zero point for each detector: (1) a reference field near the north ecliptic pole was observed immediately after cover ejection (at 12 and 25 μm, the cover was effectively at zero temperature); and (2) the detector responsivity changes caused by passage through the South Atlantic Anomaly were used to separate electronic offsets from the total detector signals at the reference field (Paper I). The results from both methods agree at 12 and 25 μm, as

expected. The estimated error in the zero-point calibrations produces uncertainty in the north ecliptic pole brightness at 12, 25, 60, and 100 μm of 5%, 20%, 25%, and 25% respectively. The absolute responsivities are also subject to uncertainties of 25% because of low-frequency effects which are not yet fully calibrated. Brightness differences in a single band between any two points on the sky are well determined and very reproducible. Spurious signals from spectral leaks, cross talk, or response to off-axis sources such as the Earth, Moon, Sun, or the satellite itself are estimated to be negligible. The conversion of observed fluxes to flux densities includes a small correction for source color temperature (Paper I).

The results presented here make particular use of data from 1983 June 24 (Fig. 1), when the scan crossed the ecliptic plane near its greatest separation (60°) from the galactic plane. At 12, 25, and 60 μm, the ZE is evidently the dominant source at this resolution except near the galactic plane. The ZE is also present at 100 μm, but diffuse galactic emission and other complex structures are prominent at this wavelength (Low *et al.* 1984). The total brightness near the ecliptic poles and at several elongations in the ecliptic plane is summarized in Tables 1 and 2. The 100 μm brightness in the February 12–21 data include a substantial galactic contribution, since these points are at low galactic latitude.

III. DISCUSSION

At high galactic latitude, the Galaxy makes an unexpectedly large contribution to the sky brightness at 100 μm. Hence, we first estimate the galactic 100 μm component and then examine the zodiacal emission.

a) Galactic Component

Figure 1 shows direct evidence of diffuse galactic emission at $|b| > 30°$ (b is galactic latitude), since the 100 μm brightness at symmetrical points on either side of the ecliptic plane is systematically higher on the side closer to the galactic plane (see also Fig. 2, Low *et al.* 1984). The brightness of this diffuse galactic emission, which we call the smooth galactic compo-
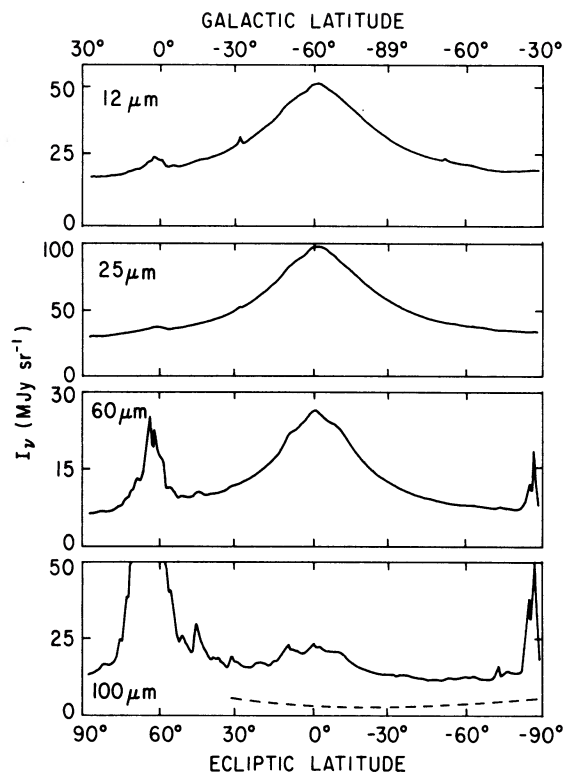
FIG. 1.—Brightness profiles for an *IRAS* scan on 1983 June 24 at elongation 91°1. The ecliptic crossing is at ecliptic longitude 1°3. The galactic plane crossing near ecliptic latitude 60° is at galactic longitude $l = 96°8$. All discrete features arise from real sources. The prominent source near the south ecliptic pole at 60 and 100 μm is the Large Magellanic Cloud. The dashed line shows our estimate of the smooth high-latitude galactic component at 100 μm.

TABLE 1

TOTAL BRIGHTNESS AT ELONGATION 91° (1983 June 24)

WAVELENGTH (μm)	FWHM	BRIGHTNESS (I_ν) (MJy sr^{-1})		
		$\beta = 88°$ $l = 95°$ $b = 28°$	$\beta = -71°$ $l = 277°$ $b = -49°$	$\beta = 0$ $l = 100°$ $b = -60°$
12	83°	18	20	51
25	68°	33	35	96
60	51°	7.2	7.8	29
100	...	12	10	21

nent, can be estimated at the galactic poles by assuming: (*a*) the ZE has the same plane of symmetry at all wavelengths; and (*b*) the diffuse galactic emission within 60° of the galactic poles varies as cosecant ($|b|$). Since the ZE symmetry plane lies nearly equidistant between the $b = -90°$ and the $b = -30°$ points in Figure 1, the difference in brightness between these two points gives approximately the galactic component at the galactic pole. Applying this argument quantitatively to data from the scans on both sides of the sky gives 2.0 and 2.4 MJy sr^{-1} at the north and south galactic poles respectively. The uncertainties in these values are -25% and $+50\%$ at each pole; these will be decreased when the ZE and the galactic emission have been accurately modeled. One implication of this result is that the minimum total 100 μm brightness should not occur at the south ecliptic pole in Figure 1, but somewhere between the south galactic and south ecliptic poles, and this is seen to be the case.

At 60 μm, repeated scans show no consistent similar asymmetry in the observed brightness. We find an upper limit on the galactic brightness at the galactic poles of approximately 0.7 MJy sr^{-1}, implying a weak upper limit on the color temperature of approximately 40 K.

The above results imply a significant amount of dust at high galactic latitude. The inferred brightness of the smooth 100 μm component is comparable to that of the cirrus clouds described by Low *et al.* (1984), suggesting that similar amounts of dust give rise to both. If the grain properties and excitation conditions of the material producing the smooth component of galactic emission and of the cirrus material are similar, then the smooth component has a color temperature of approximately 30 K. The cirrus clouds are shown by Low *et al.* to be associated with visual extinction $A_v \sim 0.1$ mag. If further study shows that the smooth high-latitude galactic component has the same properties as the cirrus clouds, then the implied visual extinction of the smooth component is also approximately 0.1 mag.

The total 100 μm emission at the south galactic pole is 13 $\pm$ 2 MJy sr^{-1}. Of this total, the smooth galactic component found above contributes 2.4 $\pm$ 1 MJy sr^{-1}, while the ZE, as shown below, contributes 4–8 MJy sr^{-1} (using a csc ($|\beta|$) law to extrapolate the ZE from the ecliptic pole, where β is ecliptic latitude). With the present zero-point uncertainties and the preliminary nature of the analysis, we can neither verify nor deny the presence of a residual 100 μm emission component for which we have not yet accounted.

TABLE 2

TOTAL BRIGHTNESS IN THE ECLIPTIC PLANE (1963 February 12–21)

WAVELENGTH (μm)	BRIGHTNESS (I_ν) (MJy sr^{-1})				
	El[a] $= 68°6$ $l = 357°$ $b = 15°$	El $= 81°5$ $l = 353°$ $b = 22°$	El $= 90°5$ $l = 351°$ $b = 25°$	El $= 98°4$ $l = 175°$ $b = -20$	El $= 103°3$ $l = 173°$ $b = -22$
12	82	59	49	43	41
25	141	105	93	82	85
60	42	38	31	27	25
100	69	73	61	47	38

[a] El = solar elongation.

b) Zodiacal Emission

In what follows, the observed brightness in the ecliptic plane and at the ecliptic poles at 12, 25, and 60 μm is interpreted as ZE. The ZE in the ecliptic plane at 100 μm is estimated by removing the galactic contribution found above from the total observed brightness. At the ecliptic poles, the high brightness apparently associated with the Galaxy (and the LMC) makes direct identification of a 100 μm ZE component quite uncertain. An estimate for the 100 μm ZE component is derived below.

i) Brightness and Spectral Energy Distribution

The ZE brightness exceeds previously published measurements at 11 and 20 μm by amounts varying from about 50% (Briotta 1976) to factors of 3–4 (Price, Murdock, and Marcotte 1980; Price, Marcotte, and Murdock 1982). Figure 2 shows the spectrum of the ZE for the ecliptic plane and the average of the ecliptic poles. The third spectrum in Figure 2 is the difference in total brightness between the ecliptic plane and a point at high ecliptic latitude ($-59°.7$) which has the same galactic latitude ($-60°$) as the ecliptic plane in this scan. Since the residual contribution of electronic offsets or galactic emission should be small, this is the least model-dependent or calibration-dependent "ZE spectrum" we can construct.

Taking account of the calibration uncertainties, these ZE spectra are fitted equally well by spectral shapes for emission from single-temperature, optically thin clouds with optical depth τ having a spectral index n of 0 or 1 ($\tau \propto \nu^n$, ν = frequency). Though the dust is not expected to be at a single temperature, the temperature and optical depth obtained from
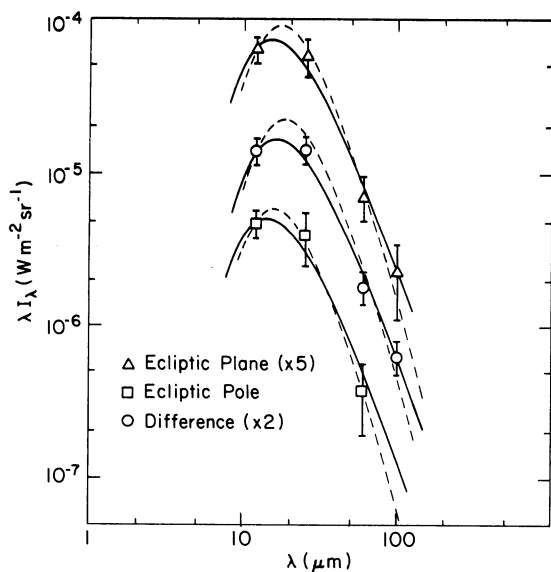
TABLE 3
ZODIACAL EMISSION TEMPERATURE AND 12 MICRON OPTICAL DEPTH

LOCATION	SPECTRAL INDEX = 0		SPECTRAL INDEX = 1	
	T (K)	τ_{12}	T (K)	τ_{12}
Ecliptic pole	275 ± 57	7.1×10^{-8}	184 ± 27	5.6×10^{-7}
Ecliptic plane ...	244 ± 44	3.0×10^{-7}	168 ± 20	2.8×10^{-6}
Difference (see text) ...	232 ± 37	2.2×10^{-7}	158 ± 16	2.4×10^{-6}

such fits provide a useful source characterization, and these are listed in Table 3. Figure 2 shows the fitted curves. In fitting the ZE spectrum at the ecliptic pole, only the data at 12, 25, and 60 μm have been included, as discussed above. The ZE brightness at 100 μm at the ecliptic pole can be estimated from these curves to lie in the range from 2 to 4 MJy sr^{-1}. For either spectral shape, the temperature at the pole is higher than that in the ecliptic plane at 91° elongation, as expected for a flattened disk distribution where the dust toward the pole is typically closer to the Sun than that seen in the disk.

ii) Geometry and Annual Modulation of the ZE

The ZE brightness at $|\beta| > 40°$ fits a cosecant ($|\beta|$) law plus a constant with residuals less' than a few percent at wavelengths shorter than 100 μm. The FWHM of the latitude distribution (Table 1) shows a systematic decrease with increasing wavelength, as expected for a flattened dust distribution with the cooler dust farther from the Sun. The FWHM is not well defined at 100 μm because the ZE is less prominent.

In the ecliptic plane, the ZE brightness is seen to decrease with increasing elongation in the range from 68° to 103° (Table 2). Fitting the spectra at these points as above gives temperatures and optical depths which decrease with increasing elongation, again qualitatively in accord with expectations.

These data have been compared quantitatively with the model calculations of Frazier (1977), who used data on visible zodiacal light and the spatial and size distributions of interplanetary dust to predict the ZE. At 12 μm, both the elongation dependence of the ZE in the ecliptic plane and its ecliptic latitude dependence at 90° elongation follow the Frazier model. Frazier's brightnesses, however, are systematically low.

Visible zodiacal light measurements have shown that the symmetry plane of the interplanetary dust is inclined with respect to the ecliptic plane by about 3°, with an ascending node near ecliptic longitude 87° (Misconi and Weinberg 1978; Leinert *et al.* 1980). The *IRAS* data support this finding, since the ecliptic poles show a difference in brightness which varies annually as expected for passage of the Earth above and below this dust symmetry plane (north brighter during the first half of the year). The fractional difference shows an amplitude of variation of about 20%, generally consistent with expectations for a dust density distribution normal to the plane varying as $\exp(-2.1z/r)$ (Leinert, Hanner, and Pitz 1978), where z is distance normal to the plane and r is distance to the Sun.

FIG. 2.—Spectra of zodiacal emission at elongation 91°.1 in the ecliptic plane and at the ecliptic pole, and a difference spectrum at points symmetrically placed with respect to the galactic pole (see text). The solid and dashed curves represent optically thin thermal emission with spectral indices n of 0 and 1 respectively ($\tau \propto \nu^n$; see Table 2).

REFERENCES

Briotta, D. A. 1976, Ph.D. thesis, Cornell University.
Frazier, E. N. 1977, *Proc. Soc. Photo-Opt. Instrum. Eng.*, **124**, 139.
Leinert C., Hanner, M., and Pitz, E. 1978, *Astr. Ap.*, **63**, 183.
Leinert, C., Hanner, M., Richter, I., and Pitz, E. 1980, *Astr. Ap.*, **82**, 328.
Low, F. J., *et al.* 1984, *Ap. J.* (*Letters*), **278**, L19.
Misconi, N. Y., and Weinberg, J. L. 1978, *Science*, **200**, 1484.

Neugebauer, G., *et al.* 1984, *Ap. J.* (*Letters*), **278**, L1 (Paper I).
Price, S. D., Marcotte, L. P., and Murdock, T. L. 1982, *A. J.*, **87**, 131.
Price, S. D., Murdock, T. L., and Marcotte, L. P. 1980, *A. J.*, **85**, 765.
Soifer, B. T., Houck, J. R., and Harwit, M. 1971, *Ap. J.* (*Letters*), **168**, L73.